Study of the plutonium (IV) electrochemical behavior in nitric acid at a platinum electrode. Application to the cathodic reduction of Pu(IV) in a plate electrolyzer

ARTICLE *in* JOURNAL OF ELECTROANALYTICAL CHEMISTRY · AUGUST 2014

Impact Factor: 2.73 · DOI: 10.1016/j.jelechem.2014.06.015

8 AUTHORS, INCLUDING:

Sébastien Picart
Atomic Energy and Alternative Energies Co…
25 PUBLICATIONS **143** CITATIONS
SEE PROFILE

Stephane Grandjean
Atomic Energy and Alternative Energies Co…
46 PUBLICATIONS **574** CITATIONS
SEE PROFILE

Jonathan Deseure
University of Grenoble
45 PUBLICATIONS **402** CITATIONS
SEE PROFILE

Journal of Electroanalytical Chemistry 727 (2014) 163–170

Contents lists available at ScienceDirect

Journal of Electroanalytical Chemistry

journal homepage: www.elsevier.com/locate/jelechem

Study of the plutonium (IV) electrochemical behavior in nitric acid at a platinum electrode. Application to the cathodic reduction of Pu(IV) in a plate electrolyzer

Sélim Georgette [a], Sébastien Picart [a,*], Christine Bouyer [b], Jérôme Maurin [a], Isabelle Bisel [a], Stéphane Grandjean [c], Jonathan Deseure [d], François Lapicque [e]

[a] RadioChemistry and Processes Department, SERA, LCAR, CEA, Nuclear Energy Division, F-30207 Bagnols-sur-Cèze, France
[b] RadioChemistry and Processes Department, SMCS, LPCP, CEA, Nuclear Energy Division, F-30207 Bagnols-sur-Cèze, France
[c] RadioChemistry and Processes Department, DIR, CEA, Nuclear Energy Division, F-30207 Bagnols-sur-Cèze, France
[d] Laboratoire d'Electrochimie et de Physicochimie des Matériaux et des Interfaces, UMR 5279 CNRS-Grenoble-INP-UJF-Université de Savoie 1130 rue de la piscine, F-38402 St Martin d'Hères, France
[e] Laboratoire Réactions et Génie des Procédés, UMR 7274 CNRS-Université de Lorraine, ENSIC, 1 rue Grandville, F-54042 Nancy, France

ARTICLE INFO

Article history:
Received 18 March 2014
Received in revised form 6 June 2014
Accepted 8 June 2014
Available online 20 June 2014

Keywords:
Plutonium
Diffusion coefficients
Charge transfer rate
Electrolysis
Platinum electrode
Nitric acid

ABSTRACT

Spent fuel reprocessing and notably plutonium recycling contributes in enhancing the sustainability of nuclear energy by preserving uranium natural resources and decreasing the long term radiotoxicity of the final waste. After initial dissolution of the spent nuclear fuel in nitric acid, uranium and plutonium recovery from ultimate waste (fission products and minor actinides) is operated by a liquid–liquid extraction process (PUREX process) and plutonium partitioning from uranium is run on the basis of the selective reduction of Pu and its back extraction. Therefore, the redox properties of Pu in nitric acid are of prime importance and the stabilization of Pu at its lower redox state + III is to be mastered. This study then deals with the characterization of Pu(IV)/Pu(III) redox couple in aqueous nitric acid solution. It was aimed at measuring physico-chemical features of the redox couple such as half-wave and conditional standard potentials, diffusion coefficients and charge transfer rate constant in nitric acid medium. These features have been used in modeling experimental results of preparative Pu(IV) reduction tests in nitrate medium in a laboratory parallel plate electrode cell.

1. Introduction

In the near-future, developed and above all emerging countries will have to meet the increasing energy needs while decreasing greenhouse gases (GHG) emissions. Regarding this challenging issue, nuclear power stands for an interesting alternative to fossil energies as it has a very low GHG-emission and produces electricity at a low and stable cost. However, nuclear energy is severely questioned after Fukushima accident and is urged to increase its efficiency in terms of safety of fuel cycle and reactors, environmental footprint and resources consumption.

Recycling the major actinides (uranium and plutonium) is to preserve uranium resources by consuming the large amount of uranium and plutonium still present in spent nuclear fuel and decreases the volume and long-term radiotoxicity of the final waste [1,2] and is no doubt the way to promote sustainability of nuclear energy. In short and mid-terms, fuel cycle has to be improved in order to optimize the actual mono-plutonium recycling in light water reactors but also to implement the future plutonium multi-recycling concomitantly to fast reactors deployment.

In the frame of the enhancement of the capability of the current spent fuel reprocessing, we have focused on the control of the valence state of plutonium which is the key factor of the uranium–plutonium partitioning [3–6]. Plutonium reduction from its stable state (+IV) to its reduced state (+III) by redox reaction with U(IV) allows its back-extraction by a nitric acid aqueous phase whereas U(IV) and U(VI) species transfer into the tributyl-phosphate organic phase [7]. The development of an electrochemical process for Pu(IV) reduction to Pu(III) species in view to extraction by nitric media appears highly interesting [8], since it would avoid the use of U(IV) reactant. This fact has motivated the determination of electrochemical data of the considered reaction at a platinum surface in nitric solutions which are still missing in

* Corresponding author. Tel.: +33 4 66 79 17 86; fax: +33 4 66 79 65 67.
E-mail address: sebastien.picart@cea.fr (S. Picart).

http://dx.doi.org/10.1016/j.jelechem.2014.06.015
1572-6657/

Nomenclature

A	electrode area (cm^2)
CV	cyclic voltammetry
D	diffusion coefficient ($cm^2\ s^{-1}$)
$E^{\circ\prime}$	conditional standard potential (V)
$E_{1/2}$	half-wave potential (V)
$E_{p,c}$ ($E_{p,a}$)	cathodic (anodic) peak potential (V)
F	Faraday number ($C\ mol^{-1}$)
I	Current (A)
j_d	limiting current density ($mA\ cm^{-2}$)
j_k	kinetic current density, in absence of mass transfer control ($mA\ cm^{-2}$)
$j_{p,c}$ ($j_{p,a}$)	cathodic (anodic) peak current density ($mA\ cm^{-2}$)
k_f	heterogeneous rate constant for reduction ($cm\ s^{-1}$)
k_m	mass transfer coefficient ($cm\ s^{-1}$)
k_s	charge transfer rate constant ($cm\ s^{-1}$)
LSV	linear sweep voltammetry
n	number of exchanged electrons (dimensionless)
NH	hydrazinium nitrate
Pt	platinum
RDE	rotating disk electrode
SCE	saturated calomel electrode
SHE	standard hydrogen electrode
v	sweep rate ($V\ s^{-1}$)
V	volume (cm^3)

Greek letters

α	charge transfer coefficient (dimensionless)
δ	diffusion layer thickness (μm)
Λ	electron and mass transfer ratio (dimensionless)
$\Psi(E_{p,c})$	quasi-reversible cathodic peak-current function (dimensionless)
ν	kinematic viscosity ($cm^2\ s^{-1}$)
ω	rotation rate ($rad\ s^{-1}$)

literature [9–13] e.g. charge transfer kinetic constant k_s and Pu(III) diffusion coefficient. Determination of a complete set of parameters for Pu(IV)/Pu(III) redox couple enabled the operating conditions of a parallel plate electrode cell for Pu(IV) reduction to be defined and to characterize the electrochemical behavior of Pu ions in terms of mass transfer.

2. Experimental

2.1. Electrochemical characterization cell and reagents

All the experiments were performed in a depressurized glove box, in order to prevent risk of contamination or irradiation due to the use of the Pu actinide, which is mainly an α emitter. The experimental setup for electrochemical investigation consisted of a small 50 cm^3 air tight vessel, thermostated at 25 °C. A three electrode configuration has been used, with a saturated calomel reference electrode (Radiometer, XR 110 model, E(25 °C) = 244 mV/*SHE*), a *Pt* wire counter-electrode (Radiometer M23PT model) and a *Pt* rotating disk electrode (Radiometer EDI 101T, 2 mm diameter and 0.031 cm^2 surface *Pt* disk). The working electrode was polished before each measurement, with lubricant diamond pastes (PRESI) with decreasing particle size from 0.2 to 0.01 μm. The solution was degassed with pure argon before analysis and gas flow was maintained during experiments.

Plutonium solutions were prepared by dilution of a stock solution of plutonium IV nitrate in a 1 mol/L nitric acid medium. The stock of plutonium solution was a 0.138 mol/L Pu(IV)$(NO_3)_4$ solution with a 1.44 mol/L free nitric acidity. Pu(IV) concentrations in the cell varied from 1 to 10 mmol/L. Hydrazinium nitrate (NH) has been used as an anti-nitrous agent and allows to stabilize Pu in its reduced oxidation state (+III) [14].

2.2. Voltammetry experiments

All measurements were performed with a Voltalab PST 050 Radiometer potentiostat or an Autolab PGSTAT 302 apparatus. The temperature was kept constant at 25 °C by use of a double-walled glass electrochemical cell. The electrode used here was a 2 mm diameter *Pt* disk, motionless or rotating at a controlled rotation speed. Cyclic voltammetry (*CV*) runs were carried out at various sweep rates v ranging from 10 to 1000 $mV\ s^{-1}$. Linear sweep voltammetry (*LSV*) with the rotating disk electrode (*RDE* Radiometer) was carried out at 2 or 5 $mV\ s^{-1}$ sweep rate and with rotating rate ω ranging from 125 and 1000 rpm. The uncompensated resistance was measured at 240 Ω by impedance spectroscopy and the ohmic drop was corrected for all scans. Curves and graphs were analyzed with Voltamaster 4, NOVA 1.9 and DIGISIM 3.0 softwares.

2.3. UV–visible absorption spectroscopy

The catholyte solution was sampled at regular intervals and was submitted to UV–visible absorption spectroscopy for analysis. As a matter of fact, as shown in Fig. 2, Pu(IV) exhibits two well defined absorption peaks at 475 and 657 nm, whereas Pu(III) stabilized by NH can be detected by its absorption at 565, 600, and 663 nm (light absorption by NH negligible in the UV–visible spectral domain). Using the spectral characteristics of Pu(IV) and Pu(III) recorded separately (Fig. 1), concentrations of the two plutonium forms in a mixture could be then determined with accuracy by factor analysis of the spectra recorded. Spectroscopic analysis of the sampled fractions made it possible to follow the progress of the electrochemical conversion along time.

2.4. Electrolysis

For application aspects, cathodic reduction of Pu(IV) solutions at preparatory scale was carried out in a parallel plate electrode

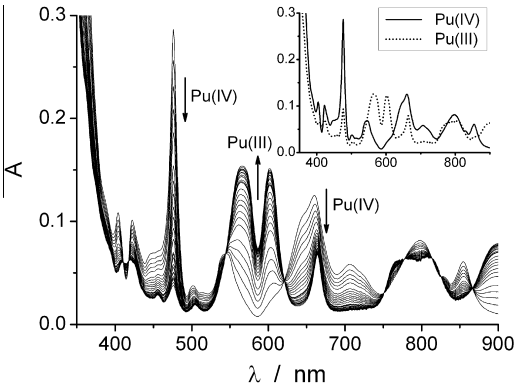

Fig. 1. Spectrophotometric monitoring of Pu(IV) and Pu(III) species during Pu(IV) electrolysis; [Pu(IV)] = 40 mM, [NH] = 0.19 M, j = 12 $mA\ cm^{-2}$, t = 0–90 min, T = 25 °C. Spectra of individual solutions are given above on the right.

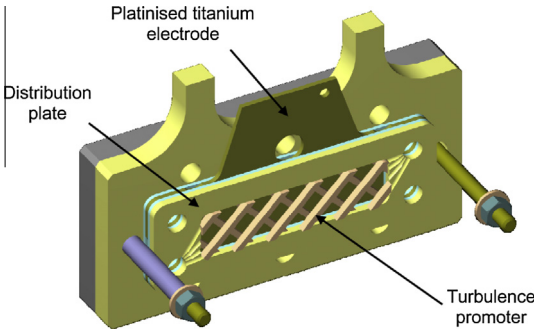

Fig. 2. Parallel plate electrode cell used for Pu(IV) solution electrolysis; here is represented a half-cell without the cationic membrane.

cell whose design is inspired from the ICI-FM01® cell, with two platinised titanium flat electrodes (12 cm^2) and two compartments separated with a Nafion® N324 cation exchange membrane. Fig. 1 gives a view of the cell. Anolyte and catholyte (1 M nitric based solutions) were circulated at same flow rate of 240 mL min^{-1} in the 6 mm thick compartment gap in presence of an inert turbulence promoter. The catholyte contained Pu(IV) at 40 mM at the beginning of the runs. Regardless of the turbulence promoter the average velocity of the flow in the cell compartments is equal to 3.33 cm s^{-1}.

3. Results and discussion

3.1. Determination of half-wave potential and Pu(IV) and Pu(III) diffusion coefficients

Linear sweep voltammetry curves recorded with Pu(IV) solutions at a concentration of 8.8 mmol/L are shown in Fig. 3a. As predicted by Levich's law, the limiting current density j_d is written as:

$$j_d = 0.62nFD^{2/3}\omega^{1/2}\nu^{-1/6}[\mathrm{Pu(IV)}] \quad (1)$$

The current density at the plateau actually varies as the square root of the rotation speed ω (Fig. 3b) and is proportional to Pu(IV) concentration (not shown here) indicating that the reduction when conducted at potentials in the range 0.4–0.2 V/*SCE* is diffusion-controlled.

The values of the current density measured at 0.3 V/*SCE* with various rotation rates and for different Pu concentrations are summarized in Table 1. The values of half-wave potentials measured in the same conditions are reported in Table 2.

Table 1
Current density measured at 0.3 V/SCE for LSV experiments with the Pt RDE under various operating conditions: [Pu(IV)] = 1–10 mmol/L; ω = 125–2000 rpm. Scan rate ν was fixed at 2 mV s^{-1} and experiments were carried out at 25 °C.

	$\lvert j_d\rvert$ (μA cm^{-2})			
ω (rpm)/[Pu] (mmol/L)	1.0	5.0	8.8	10
100	/	/	2.7 ± 0.1	/
125	0.33 ± 0.02	1.7 ± 0.1	/	3.4 ± 0.3
250	0.47 ± 0.04	2.3 ± 0.1	4.1 ± 0.2	4.7 ± 0.3
500	0.64 ± 0.07	3.3 ± 0.2	5.8 ± 0.3	6.4 ± 0.4
1000	0.86 ± 0.09	4.5 ± 0.2	8.0 ± 0.4	8.9 ± 0.5
2000	/	/	11.1 ± 0.5	/

Table 2
Experimental half-wave potential values of Pu(IV) reduction at 25 °C by linear sweep voltammetry for various Pu concentrations and rotation rates.

ω (rpm)/[Pu] (mmol/L)	$E_{1/2}$ (mV vs. *SCE*)			
	1.0	5.0	8.8	10
100	/	/	677	/
125	685	684	/	680
250	680	678	671	674
500	677	677	668	668
1000	667	673	677	663

According to the conventional relation between potential and current density for reversible couples (Eq. (2)) [15], plotting the potential value E vs. $\log((j_d-j)/j)$ is to yield a linear relationship between the two variables: the slope is reciprocal to the number of electrons exchanged and the intercept with the ordinate axis yields the half-wave potential $E_{1/2}$.

$$E = \frac{2.3RT}{nF}\log\left(\frac{j_d - j}{j}\right) + E_{1/2} \quad (2)$$

Fig. 4 compares the experimental voltammetric variations to the theoretical voltage assuming $n = 1$.

Fitting the experimental data after Eq. (2) obtained with various Pu(IV) solutions and at various rotation rates showed that the number of electrons exchanged in the reduction n was equal to 0.97 ± 0.07. This value does not significantly differ from the theoretical value at one, which confirms that the electrochemical couple was actually Pu(IV)/Pu(III).

The half-wave potential of Pu(IV)/Pu(III) couple in nitric medium was determined at: $E_{1/2}(Pu^{IV}/Pu^{III})$ = 676 ± 6 mV/*SCE* = 920 ± 9 mV/*SHE* at 25 °C.

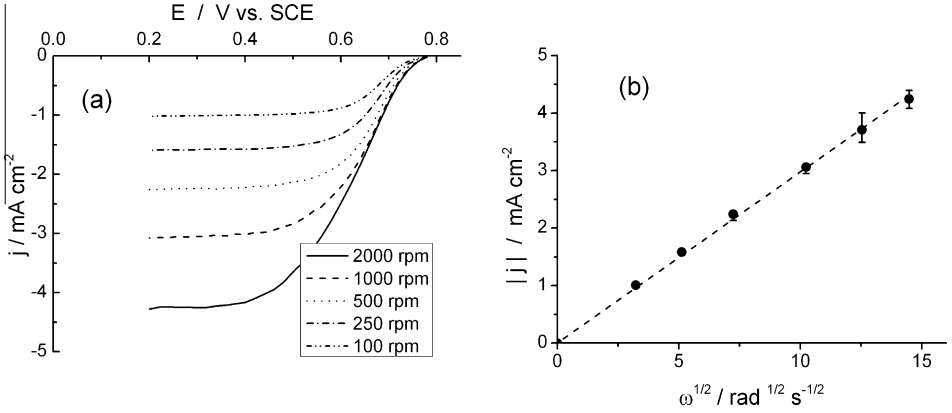

Fig. 3. (a) Current density potential curves of a 8.8 mmol/L Pu(IV) solution in 1 mol/L nitric acid at a rotating Pt disk electrode, with various rotation rates; ν = 2 mV s^{-1}; T = 25 °C. (b) Levich plot of the current density measured at 0.3 V/SCE vs. the square root of rotation rate ω.

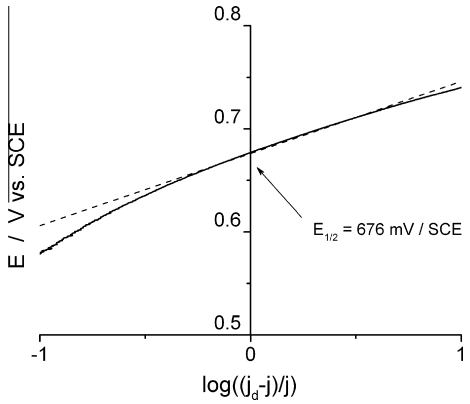

Fig. 4. Electrode potential vs. $\log(j_d-j)/j$ from LSV experiments (solid line) compared to the theoretical potential calculated after Eq. (2) and assuming a single-electron exchange system (dotted line). [Pu(IV)] = 8.8 mmol/L; ω = 100 rpm; v = 2 mV s^{-1}; T = 25 °C.

This estimate is consistent with the average value of $E_{1/2}$ = 677 ± 5 mV/*SCE* which can be deduced from Table 2, and with previously reported values [11,14,16].

Levich plot (Fig. 3b) obtained for different Pu concentrations allowed the determination of the diffusion coefficient of Pu(IV). The kinematic viscosity ν was measured at 9.12×10^{-3} cm^2 s^{-1} at 25 °C – this value has been used here. The Pu(IV) diffusion coefficient was then found to be equal to $(4.6 \pm 0.5)\ 10^{-6}$ cm^2 s^{-1}, which is in good agreement with already published data for nitric acid medium [10] (see Table 3).

The determination of Pu(III) diffusion coefficient by linear sweep voltammetry (*LSV*) – or by any electrochemical technique – requires the preparation of Pu(III) solution. This species is unstable in the presence of nitrous acid, even present at trace concentration in equilibrium with concentrated nitric acid (around 10^{-4} mol/L) [17]. Addition of anti-nitrous agents e.g. hydrazine as usually carried out, cannot be considered here because these agents interfere in the anodic process. Therefore the Pu(III) solutions were characterized by linear sweep voltammetry immediately after preparative reduction in the parallel plate electrode cell. Electrochemical reduction runs were carried out in galvanostatic mode at a current density of 12 mA cm^{-2} during 20 min.

This solution was first characterized by absorption spectrophotometry to determine Pu(III) concentration; the current – potential curve was recorded immediately afterwards at the above *RDE*, to neglect Pu(III) re-oxidation [18]. The limiting current densities were thus measured for different Pu(III) concentrations and at different rotation rates of the disk electrode. From those results, plotting limiting current density ratios j_d/[Pu(III)] vs. the square root of rotation rate gave a linear relation which slope allowed estimation of the Pu(III) diffusion coefficient (Fig. 5). This diffusion coefficient was found at $D_{Pu(III)} = (6.2 \pm 0.7)\ 10^{-6}$ cm^2 s^{-1}. This value is significantly higher than the published values [10,19] and slightly stronger than the diffusion coefficient of Pu(IV) (Table 3).

Table 3
Diffusion coefficient of Pu(IV) and Pu(III) in acidic solutions at 25 °C: comparison of the obtained values to literature data.

Specie	Medium	Technique	$D/10^{-6}$ cm^2 s^{-1}	Refs.
Pu(III)	H_2SO_4 0.5 M	Chronopot.	4.7 ± 0.1	[10]
Pu(III)	H_2SO_4 0.5 M	Voltammetry	3.0	[19]
Pu(III)	HNO_3 0.5 M	Voltammetry	3.3	[19]
Pu(III)	HNO_3 1 M	Voltammetry	6.2 ± 0.7	Present work
Pu(IV)	HCl 1 M	Chronopot.	5.2 ± 0.2	[10]
Pu(IV)	$HClO_4$ 1 M	Chronopot.	4.7 ± 0.1	[10]
Pu(IV)	HNO_3 1 M	Chronopot.	5.8 ± 0.1	[10]
Pu(IV)	H_2SO_4 0.5 M	Chronopot.	5.0 ± 0.1	[10]
Pu(IV)	HNO_3 1 M	Voltammetry	1.19	[11]
Pu(IV)	HNO_3 1 M	Voltammetry	5.6 ± 0.2	[12]
Pu(IV)	HNO_3 1 M	Voltammetry	4.6 ± 0.5	Present work

3.2. Assessment of the conditional potential

The conditional potential actually differs slightly from the half-wave potential $E_{1/2}$, as shown by Eq. (3) [20]. This potential could be estimated from the experimental values of the half wave potential and the diffusion coefficients of Pu(IV) and Pu(III).

$$E_{1/2} = E^{\circ\prime} + \frac{RT}{nF} \ln \left(\frac{D_{Pu(III)}}{D_{Pu(IV)}} \right)^{2/3} \quad (3)$$

The values obtained, given hereafter, $E^{\circ\prime}$(Pu(IV)/Pu(III)) = 678 ± 6 mV/*SCE* = 922 ± 6 mV/*SHE* at 25 °C in HNO_3 1 mol/L are in good agreement with data taken from literature as shown in Table 4:

3.3. Estimation of the kinetic constant of electron transfer

According to cyclic voltammetry experiments run for Pu(IV) solutions, cathodic peak current densities $j_{p,c}$ are proportional to the square root of potential scan rate (see Fig. 6) which is in accordance with Randles-Sevcick theory applied to planar semi-infinite diffusion conditions:

$$j_{pc} = \Psi(E_{p,c}) \sqrt{\frac{nF\nu D}{RT}} nF[\mathrm{Pu(IV)}]_{bulk} \quad (4)$$

where the proportionality factor $\Psi(E_{p,c})$ is discussed below. The above proportionality indicates that diffusion rate dominates the overall rate of the process more than the rate of electron transfer [21].

However, it appears from Fig. 6a that the difference between the anodic and cathodic peak potentials ($E_{p,a}$–$E_{p,c}$) is larger than the theoretical difference at 59 mV for a single-electron perfectly reversible process at 25 °C – the experimental differences are reported in Table 5. Moreover the profile of the current density variation with the square root of the scan rate is not perfectly linear (Fig. 6b): the slope of the variation decreases somehow at high scan rates. As a matter of fact, the $\psi(E_p)$ term appearing in Eq. (4) was shown to lie between 0.446 – for reversible systems, if α = 0.5 – and 0.351 with irreversible systems [20,22] (Fig. 7). This indicates a mixed control system and a quasi-reversible charge transfer: for low scan rates, the electrochemical system appears as reversible since the electrode response can easily follow the potential scan. In contrast, for the highest scan rate, the electrode response is strongly affected by the transient regime, so the electrode reaction can be considered as mainly irreversible, with lower peak current densities. This transitional regime is confirmed by the above deviation of potential difference ($E_{pa} - E_{pc}$) for the theoretical 59 mV: the reduction is not a fully reversible process, and is considered here as a quasi-reversible process.

Moreover a new estimation of $E_{1/2}$ for Pu(IV)/Pu(III) redox couple can be obtained by the mean value of the potential peaks: the data obtained (Table 5) are in good agreement with the data discussed above.

Numerical simulation with DIGISIM 3.0®, based on implicit finite difference formulation of kinetic diffusion mass balance in electrochemistry [23,24], was then used to fit the voltammetric data and to extract the charge transfer kinetic constant k_s, knowing the diffusion coefficient of Pu(IV) and Pu(III) and conditional standard potential $E^{\circ\prime}$, and assuming a quasi-reversible process and a transfer coefficient α equal to 0.5 – corresponding to a symmetric energy profile.

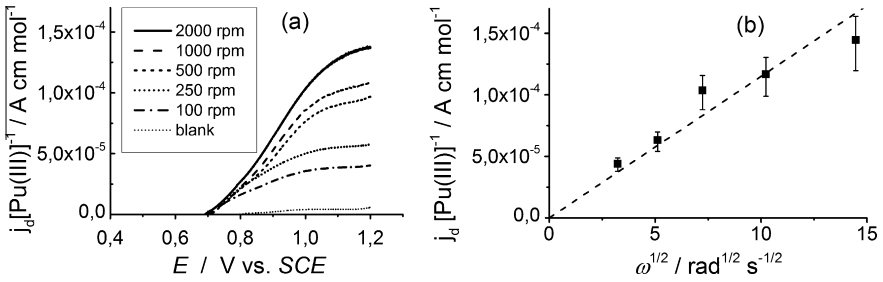

Fig. 5. Levich plot of the limiting current (measured at E = 1.1 V vs. SCE) over Pu (III) concentration vs. square root of rotation rate; $[Pu]_{tot}$ = 8.8 mmol/L; Pt electrode; ω = 100–2000 rpm; v = 2 mV s^{-1}; T = 25 °C.

Table 4
Conditional standard potentials of plutonium (IV) and plutonium (III) redox pair in a 1 mol/L nitric acid. Comparison with literature data. Potentials are given in mV/SHE.

$[HNO_3]$ (mol L^{-1})	Our work	[21]	[12]
0.75		938.7 ± 1.5	–
1.00	922 ± 6	932.2 ± 0.6	923
1.25		928.3 ± 1.6	–
1.50		923.1 ± 1.7	–
2.00		908.6 ± 1.5	934

Table 5
Anodic and cathodic peak potentials, corresponding half-wave potentials and difference of peak potentials given in mV/*SCE*. [Pu(IV)] = 8.8 mmol/L; Pt electrode; S = 0.031 cm^2; v = 25–250 mV s^{-1}; T = 25 °C.

v (mV s^{-1})	E_{pc} (mV)	E_{pa} (mV)	$E_{1/2} = (E_{pa} + E_{pc})/2$ (mV)	ΔE_p (mV)
25	638 ± 5	726 ± 5	682 ± 5	88 ± 5
50	633 ± 5	733 ± 5	683 ± 5	100 ± 5
100	630 ± 5	735 ± 5	682 ± 5	105 ± 5
250	622 ± 5	742 ± 5	682 ± 5	120 ± 5

Fitting of the experimental data at different scan rates led to a charge transfer kinetic constant k_s, at $3.5 \times 10^{-3} \pm 0.5$ cm s^{-1}. The constant value is nearly ten times larger than the rate constant determined by Kim and co-workers [12] at glassy carbon electrode ($k_s = 0.398 \times 10^{-3}$ cm s^{-1}): the deviation can be explained by the far better catalytic properties exhibited by platinum for the reduction in comparison to glassy carbon materials, with lower electrical activation energy with platinum than with carbon electrode [20].

Fig. 8 illustrates the agreement between experimental and calculated variations, for the determined value of k_s.

Parameter Λ, defined in Eq. (5),

$$\Lambda = k_s \Big/ \left[D_{Pu(III)}^{1-\alpha} D_{Pu(IV)}^{\alpha} \left(\frac{nF}{RT}\right) v \right]^{1/2} \quad (5)$$

compares the rates of electron and mass transfer for a given scan rate [17]. This criterion was calculated for $D_{Pu(III)} = 6.2 \times 10^{-6}$ cm^2 s^{-1} and $D_{Pu(IV)} = 4.6 \times 10^{-6}$ cm^2 s^{-1} (see Table 3). For the range of scan rate investigated, this criterion varies between 0.8 and 3, corresponding to a quasi-reversible regime ($15 \geqslant \Lambda \geqslant 10^{-2(1+\alpha)}$) [25] which confirms the assumption made in the simulation.

Besides, data from linear sweep voltammetry can also be used as a second method to determine rate constant k_s. This method is based on the determination of kinetic current j_k at different potential for non-limiting current conditions [20]: the current density is expressed as a function of j_k, the kinetically controlled current density and j_d, diffusion-controlled limiting current density. At a rotating disk electrode, the current density j is written as:

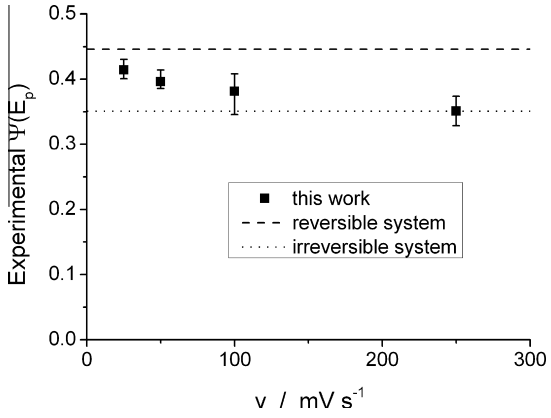

Fig. 7. Proportionality factor $\psi(E_p)$ vs. the scan rate for [Pu(IV)] = 8.8 mmol/L. The dotted lines are theoretical values for reversible and irreversible systems [20,22].

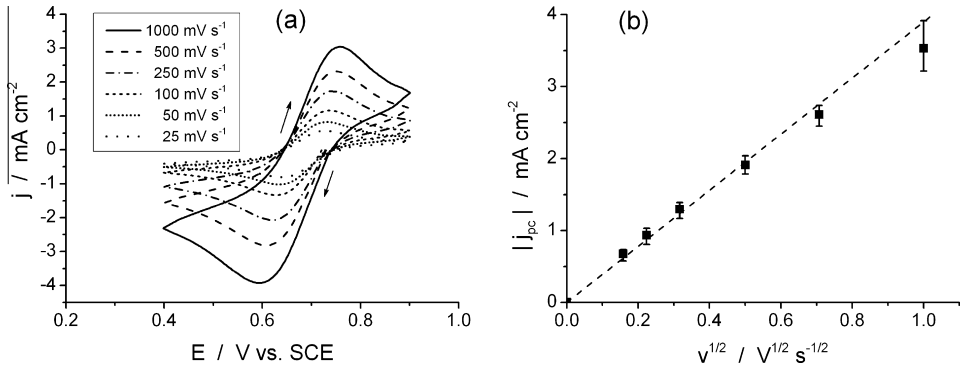

Fig. 6. (a) Cyclic voltammetry of a 8.8 mmol/L Pu(IV) solution at various potential scan rates. v = 25–1000 mV s^{-1}; T = 25 °C. (b) Cathodic peak current density vs. the square root of the scan rate; the dotted line corresponds to the average linear variation.

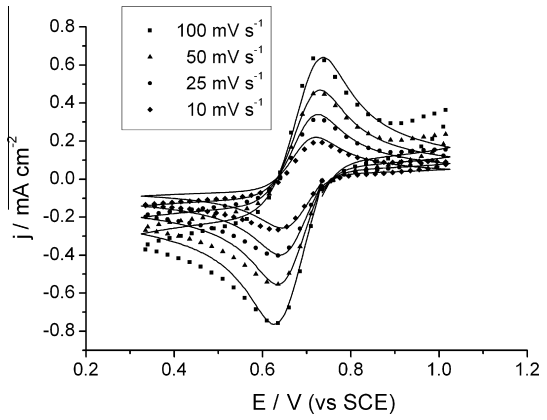

Fig. 8. Simulated and experimental cyclic voltammograms of a 5 mmol/L Pu(IV) solution in HNO_3 1 M medium; $k_s = 3.5 \times 10^{-3}$ cm s^{-1}; $D_{Pu(IV)} = 4.5 \times 10^{-6}$ cm^2 s^{-1}; $D_{Pu(III)} = 6.2 \times 10^{-6}$ cm^2 s^{-1}; $v = 10$–100 mV s^{-1}; $T = 25$ °C; solid lines are for simulation, symbols are for experimental data.

$$\frac{1}{j} = \frac{1}{j_k} + \frac{1}{j_d} = \frac{1}{j_k} + \frac{1}{0.620nF[\mathrm{Pu(IV)}]D_{\mathrm{Pu,(IV)}}^{2/3}\nu^{-1/6}\omega^{1/2}} \quad (6)$$

Plot of the reciprocal of the current density vs. the reciprocal of the square root of the rotation rate ω, for a given potential results in linear variations, as demonstrated in Fig. 9a. The slope corresponds to the factor $0.620nF[\mathrm{Pu(IV)}]D_{\mathrm{Pu(IV)}}^{2/3}\nu^{-1/6}$ (Eq. (6)) and the extrapolation of $1/j$ at the ordinate axis yields $1/j_k$. Determination of j_k at different values of E then allows determination of the kinetic parameters k_s by fitting the variation of j_k with E according to Eq. (7). In the case of a quasi-reversible system, we have to consider the forward and backward currents densities (Butler–Volmer law [20]).

$$j_k = nFk_s\left(-\exp\left[-\frac{\alpha nF(E-E^{\circ\prime})}{RT}\right][\mathrm{Pu(IV)}] + \exp\left[\frac{(1-\alpha)nF(E-E^{\circ\prime})}{RT}\right][\mathrm{Pu(III)}]\right) \quad (7)$$

In the present case – $\alpha = 0.5$ and the potential differences $|E–E^{\circ\prime}|$ are larger than 80 mV – the second exponential term could be neglected, giving the simplified expression below:

$$j_k \approx nFk_f[\mathrm{Pu(IV)}] \quad (8)$$

With

$$k_f = k_s \exp\left[-\frac{\alpha nF(E-E^{\circ\prime})}{RT}\right] \quad (9)$$

The value of k_s estimated by the Tafel plot in Fig. 9b was found at $3.0 \pm 0.5 \times 10^{-3}$ cm s^{-1}, in good agreement with previous determination at $3.5 \pm 0.5 \times 10^{-3}$ cm s^{-1}, which validates the model employed for fitting the *CV* assuming a quasi-reversible system. The final k_s value was taken as the average of these two estimations at 3.3×10^{-3} cm s^{-1}.

4. Electrolysis of Pu(IV) solution

A test for Pu(III) generation was carried out in the parallel plate electrode cell to demonstrate that the quantitative cathodic reduction of Pu(IV) was feasible in molar nitric acid solutions in the presence of an anti-nitrous agent.

4.1. Experimental results

The quantitative reduction of Pu(IV) solutions ($V = 30$ cm^3) was carried out either in current or potential controlled mode in the separated plate electrode cell. The two main reactions involved are the reduction of Pu(IV) and the oxidation of H_2O, in the cathodic and anodic compartments respectively.

$$Pu^{4+} + e^- \rightarrow Pu^{3+} \quad E^{\circ\prime} = 0.68\ \mathrm{V}/SCE\ (1\ \mathrm{M\ HNO_3},\ I = 1\ \mathrm{M},\ T = 25\ ^\circ\mathrm{C})$$

$$H_2O \rightarrow 1/2O_2 + 2H^+ + 2e^- \quad E^\circ = 1.23\ \mathrm{V}/NHE \approx 0.99\ \mathrm{V}/SCE\ (\mathrm{pH} = 0,\ I = 0\ M,\ T = 25\ ^\circ\mathrm{C})$$

Nitrate reduction to nitrous acid can be considered negligible since no accumulation of nitrous acid could be evidenced (below the detection limit at 10^{-4} mol L^{-1}) in the course of nitric acid electrolysis. For experiments at fixed current density the initial Pu concentration was 40 mmol/L and hydrazinium nitrate was added as anti-nitrous agent at 200 mmol/L (large excess). Assuming a mass transfer coefficient at 10^{-3} cm s^{-1}, the limiting current density of Pu(IV) can be estimated using Eq. (8) [20]:

$$j_d = nFk_m[\mathrm{Pu(IV)}] \quad (10)$$

Estimation for diffusion current density is near 4 mA cm^{-2}. NB: from the diffusion coefficient of Pu(IV) species equals to 4.6×10^{-6} cm^2 s^{-1}, the thickness of Nernst diffusion layer is equal to 46 μm, which is of expectable order of magnitude.

The average current density was fixed at 12 mA cm^{-2}, noticeably larger than the above estimated limiting current density. The cell voltage was always higher than 2 V (see Fig. 10), which indicates that the cathode potential was presumably far more negative than the Pu(IV)/Pu(III) conditional potential (0.68 V/*SCE*) if

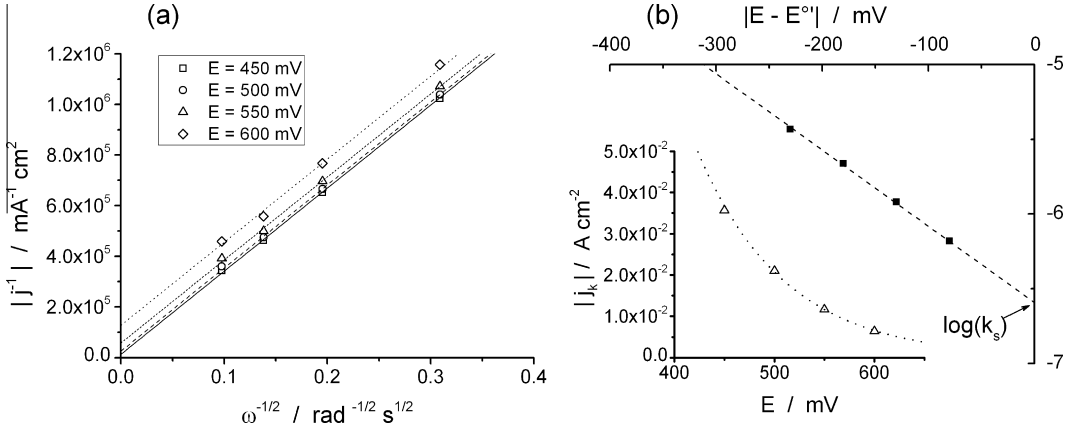

Fig. 9. (a) Reciprocal of the current density vs. the reciprocal of the square root of rotation rate; (b) Variation of the kinetically limited current density with the electrode potential and k_s determination; [Pu(IV)] = 8.8 mmol/L in HNO_3 1 mol/L; $\omega = 100$–1000 rpm; $v = 2$ mV s^{-1}; $T = 25$ °C; $E^{\circ\prime} = 678$ mV vs. SCE.

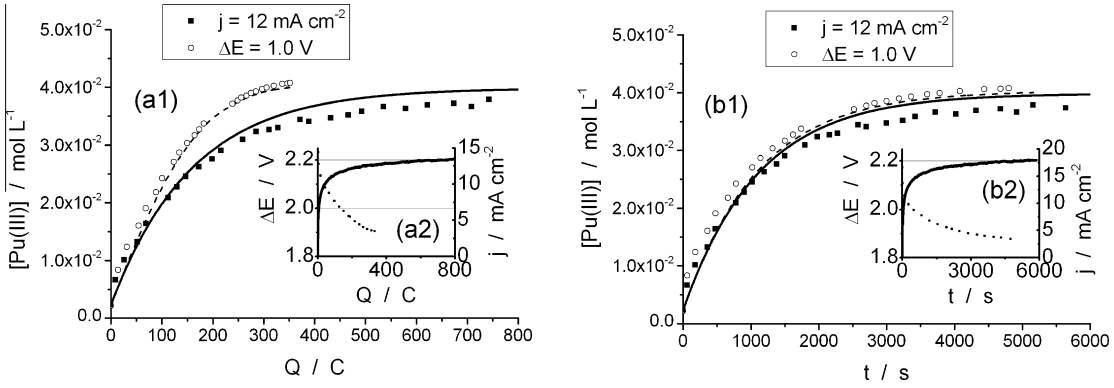

Fig. 10. Electrolysis of a Pu(IV) solution (a1–b1) Reduction kinetics: (symbols) experimental data at fixed current (■) and potential (○), (solid line) calculated variations; (a2–b2) cell voltage (solid line) and cell current (dotted line) recorded during electrolysis at fixed current and difference of potential respectively.

one assumes that the anode potential for O_2 evolution on the platinised surface does not exceed 1.75 V/*NHE*, i.e. approx. 1.51 V/*SCE*: although oxygen evolution is known to be a slow reaction, even at platinised electrodes [26,27]. According to Conway et al. [27] for current density close to 12 mA cm^{-2} the overall voltage of the platinised anode for oxygen evolution should not exceed 500 mV: although oxygen evolution is a slow reaction, the anode potential can be considered as not being over 1.51 V/*SCE*. Therefore, the cathode potential is presumably below 0 V/*SCE*, far more negative than the Pu(IV)/Pu(III) conditional potential (0.68 V/*SCE*), and the reduction could be considered as diffusion-controlled.

The progress in Pu(IV) reduction was followed by UV–visible spectrophotometry which could yield the time variation of Pu(III) concentration (Fig. 10). The reduction was nearly quantitative and conversion rates could reach 94% within 90 min. The faradaic efficiency was only at 15%, confirming the significance of side reactions, in particular hydrogen evolution.

Experiments were also carried out at a fixed cell voltage of 1 V. This value was chosen higher than the difference of potentials for Pu(IV) reduction and H_2O oxidation, considering that the anode potential for O_2 evolution does not exceed 1.51 V/*SCE* and using the Pu(IV)/Pu(III) reduction conditional potential. The initial Pu concentration was 42 mmol/L and the initial hydrazinium nitrate concentration (*NH*) was 0.2 mol/L. A 98% conversion yield was achieved within 85 min and the current efficiency attained 35%. The times for next-to complete reduction in the two operating modes are comparable in spite of very different profiles of current density: this indicates that the reduction of Pu(IV) was carried out under diffusion controlled in the two cases.

As expected, faradaic efficiency is higher for the controlled potential mode because the cathodic potential is presumably less reductive than at the selected fixed current density, so proton reduction occurs with quite a lower extent (see Fig. 10(a1)). The optimal mode is then a control potential electrolysis with a fixed cell voltage equal or below 1 V.

4.2. Modeling for mass transfer control

For the experiments carried out at 12 mA cm^{-2}, and the reasons given above, reduction can be considered as diffusion controlled, then the current density varies linearly with Pu(IV) concentration according to Eq. (9).

$$J_{Pu}(t) = nFk_m[\mathrm{Pu(IV)}]_t \tag{11}$$

The time variation of Pu(III) concentration can be calculated by integrating the following kinetic relation (Eq. (10)).

$$\frac{d[\mathrm{Pu(III)}]}{dt} = \frac{I(t)}{nFV} = \frac{Ak_m}{V}[\mathrm{Pu(IV)}]_t \tag{12}$$

Considering $[\mathrm{Pu(IV)}]_t = [\mathrm{Pu(IV)}]_{t=0} - [\mathrm{Pu(III)}]_t$ and $[\mathrm{Pu(III)}]_{t=0} = 0$, then Eq. (10) can be integrated analytically:

$$[\mathrm{Pu(III)}]_t = [\mathrm{Pu(IV)}]_{t=0}\left(1 - \exp\left(-\frac{Ak_m}{V}t\right)\right) \tag{13}$$

The calculated time variation of Pu(III) concentration was fitted to the experimental data, which allowed mass transfer coefficient k_m to be estimated at 2.2×10^{-3} cm s^{-1}; and the theoretical curve to be plotted in Fig. 10(b1) as a function of time and charge (Fig. 10(a1)). The determined mass transfer coefficient k_m is of the same order of magnitude than the simulated one in the FM01-LC electrolyzer, obtained by simulation by Rivero et al. [28] near 2.5×10^{-4} cm s^{-1} with an average flow velocity of 0.85 cm s^{-1} (in our study the average flow velocity equals 3.33 cm s^{-1}): the difference could be due to different flow velocity and mesh of the turbulence promoter.

For the experiment at fixed cell voltage, assuming that the charge transfer rate k_f remains constant along the run, the general current expression for a mixed control is given in Eq. (12).

$$I = \frac{nFAk_f[\mathrm{Pu(IV)}]}{1 + k_f k_m} \tag{14}$$

where k_f is defined thereby:

$$k_f = k_s \exp\left[-\frac{\alpha nF(E_c - E^{\circ\prime})}{RT}\right] \tag{15}$$

E_c is the cathodic potential obtained from the measured difference of potential and the anodic pseudo-potential corresponding to O_2 evolution estimated at 0.99 V/*SCE* in the case of a potentiostatic mode with an 1.0 V applied tension, i.e. E_c = 0.01 V/*SCE*. Value of k_f was estimated at 5.0×10^5 cm s^{-1} using the determined k_s value, i.e. nearly 10^7 times larger than k_m estimate which confirms that the diffusion controlled operation, also for the run conducted at 1 V.

5. Conclusion

This study was aimed at determining the physicochemical parameters of Pu(IV)/Pu(III) redox pair at a platinum electrode in molar nitric acid. Some of the parameters estimated such as Pu(IV) diffusion coefficient and conditional potential are in good agreement with formerly published data whereas the value of Pu(III) diffusion coefficient was found to be significantly higher than the published value (6.2×10^{-6} cm^2 s^{-1} vs. 3.3×10^{-6} cm^2 s^{-1} [19]). This investigation could also provide an estimation of the electron transfer constant $k_s = 3.3 \times 10^{-3}$ cm s^{-1} for the reduction at a platinum electrode: this value is nearly one order of magnitude higher than the previous determination at glassy carbon electrode by Kim

et al. [12], but the deviation can be attributed to the very different catalytic properties of the two materials. In spite of its cost, platinum appears as suitable for Pu(IV) reduction. Eventually, those data helped interpreting the performance of the plate electrode cell used batchwise for Pu(III) generation: the reduction can be operated under mass transfer control, but operations at controlled cell voltage are to be preferred for the sake of higher faradaic efficiency along the batch run.

Conflict of interest

There is no conflict of interest.

Acknowledgements

The authors thank AREVA NC for financial support of this study.

References

[1] C. Poinssot, B. Boullis, Nucl. Eng. Int. 57 (2012) 17.
[2] C. Poinssot, C. Rostaing, S. Greandjean, B. Boullis, Atalante 2012 International Conference on Nuclear Chemistry for Sustainable Fuel Cycles, 7 (2012) 349, http://dx.doi.org/10.1016/j.proche.2012.10.055.
[3] C. Madic, M. Lecomte, P. Baron, B. Boullis, C.R. Phys. 7–8 (2002) 797–811, http://dx.doi.org/10.1016/S1631-0705(02)01370-1, ISSN 1631-0705.
[4] M. Bourgeois, Retraitement du combustible – Principales opérations, Techniques de l'ingénieur Cycle du combustible nucléaire: combustibles usés et déchets radioactifs, Paris, 2000, BN 3650.
[5] J.J. Katz, G.T. Seaborg, L.R. Morss, The Chemistry of The Actinide Elements, vol. 1, Chapman and Hall, London, 1986, ISBN 0-412-10550-0.
[6] V.N. Kosyakov, V.I. Marchenko, Radiochemistry 50 (2008) 333–345, http://dx.doi.org/10.1134/S1066362208040012, ISSN 1608-3288.
[7] B. Bonin, E. Abonneau, I. Bisel, C. Den Auwer, et al., Le traitement-recyclage du combustible nucléaire usé: La séparation des actinides, application à la gestion des déchets, Le Moniteur Editions, Paris, 2008, ISBN 978-2-281-11376-1.
[8] M. Borland, S. Frank, B. Patton, B. Cowell, K. Chidester, An evaluation of alternate production methods for Pu-238 general purpose heat source pellets, in: Proceedings of Nuclear and Emerging Technologies for Space, Atlanta, GA, 2009, OSTI 974750.
[9] D.G. Peter, W.D. Shults, J. Electroanal. Chem. 8 (1964) 200–229, http://dx.doi.org/10.1016/0022-0728(64)80115-7, ISSN 0368-1874.
[10] S. Casadio, F. Orlandini, J. Electroanal. Chem. Interfacial Electrochem. 33 (1971) 212–215, http://dx.doi.org/10.1016/S0022-0728(71)80224-3, ISSN 0022-0728.
[11] S.Y. Kim, T. Asakura, Y. Morita, J. Radioanal. Nucl. Chem. 295 (2013) 937–942, http://dx.doi.org/10.1007/s10967-012-1858-z, ISSN 0236-5731.
[12] H.M. Steele, D. Guillaumont, P. Moisy, et al., J. Phys. Chem. A 117 (2013) 4500–4505, http://dx.doi.org/10.1021/jp401875f, ISSN-5639. ISSN 1089-5639.
[13] S. Kihara, Z. Yoshida, H. Aoyagi, K. Maeda, O. Shirai, Y. Kitatsuji, Y. Yoshida, Pure Appl. Chem. 71 (1999) 1771–1807, http://dx.doi.org/10.1351/pac199971091771, ISSN 0033-4545.
[14] J.R. Perron, G. Stedman, N. Uysal, J. Chem. Soc., Dalton Trans. 20 (1976) 2058–2064, http://dx.doi.org/10.1039/DT9760002058.
[15] H.H. Girault, Electrochimie physique et analytique, PPUR presses polytechniques, Lausanne, 2007, ISBN 9782880746735.
[16] K. Koyama, Anal. Chem. 4 (1960) 523–524, http://dx.doi.org/10.1021/ac60160a020, ISSN 0003-2700.
[17] N.N. Andreychuk, A.A. Frolov, K.V. Rotmanov, V.Y. Vasiliev, J. Radioanal. Nucl. Chem. Art. 143 (1990) 427–432, http://dx.doi.org/10.1007/BF02039611, ISSN 0236-5731.
[18] V.S. Koltunov, V.I. Marchenko, Radiokhimiya 15 (1973) 777–781. UDC 541.127:546.799.4:546.173.
[19] C.E. Plock, Anal. Chim. Acta 49 (1970) 83–87, http://dx.doi.org/10.1016/S0003-2670(01)80010-6, ISSN 0003-2670.
[20] A.J. Bard, L.R. Faulkner, Electrochemical Methods Fundamentals and Applications, Wiley, New-York, 1980, ISBN 0-471-05542-5.
[21] A.G. Wain, The potential of the Pu(III)-Pu(IV) couple in nitric acid solution and equilibrium constants for the nitrato complexes of Pu(IV), U.K. Atomic Energy Research Establishment, 7110 (1966), OSTI 4074095.
[22] F. Scholz, Electroanalytical Methods: Guide to Experiments and Applications, Springer, Berlin, 2010, ISBN 9783642029158.
[23] M. Rudolph, J. Electroanal. Chem. Interfacial Electrochem. 314 (1991) 13–22, http://dx.doi.org/10.1016/0022-0728(91)85425-O, ISSN 0022-0728.
[24] M. Rudolph, J. Electroanal. Chem. Interfacial Electrochem. 338 (1992) 85–98, http://dx.doi.org/10.1016/0022-0728(92)80415-Z, ISSN 1572-6657.
[25] H. Matsuda, Y. Ayabe, Zeitschrift Fur Elektrochemie 59 (1955) 494–503.
[26] L.B. Kriksunov, L.V. Bunakova, S.E. Zabusova, L.I. Krishtalik, Electrochim. Acta 39 (1994) 137–142, http://dx.doi.org/10.1016/0013-4686(94)85020-8.
[27] B.E. Conway, T.C. Liu, Mater. Chem. Phys. 22 (1989) 163–182, http://dx.doi.org/10.1016/0254-0584(89)90036-9, ISSN 0254-0584.
[28] E.P. Rivero, F.F. Rivera, M.R. Cruz-Díaz, E. Mayen, I. González, Chem. Eng. Res. Des. 90 (2012) 1969–1978, http://dx.doi.org/10.1016/j.cherd.2012.04.010, ISSN 0263-8762.